PHYSICAL REVIEW A VOLUME 4, NUMBER 1 JULY 1971

Asymptotic Line Shape in Collision-Induced Light Scattering

Joel I. Gersten
Department of Physics, City College of the City University of New York, New York, New York 10031
(Received 6 October 1970)

A theory for the spectral wings of collision-induced scattered light is presented. It differs from previous theories in that realistic potentials and polarizabilities are employed. The line shape at relatively low frequencies is determined largely by the effects of distant collisions. At high frequencies it is determined primarily by the repulsive part of the interatomic potential. At intermediate frequencies it is sensitive to both the attractive part of the potential and the short-range part of the polarizability anisotropy. A technique in which the analytic behavior of the trajectories in the complex time plane plays a key role is employed.

INTRODUCTION

Recent investigations of collision-induced optical phenomena at low densities have revealed a close connection between conventional molecular spectra and pressure-induced spectra. Corresponding to the infrared-allowed transitions of molecular spectroscopy there exists collision-induced absorption. Isolated atoms are not able to absorb infrared radiation via electric dipole transitions but heterogeneous pairs of atoms may. Corresponding to vibrational or rotational transitions in a true molecule there exist translational (radial or tangential) momentum changes. The analog of Raman scattering is collision-induced light scattering (CIS). Whereas isolated atoms are not capable of changing the polarization of incident light, interacting pairs of atoms may do so. In analyzing pressure-induced processes one may regard the pair of atoms as forming a quasimolecule which lasts the duration of a collision. In such a description the analogy with molecular spectroscopy is apparent.

Theoretical studies of CIS spectra have been made recently by Levine and Birnbaum[1,4] and Thibeau and Oksengorn.[2] In the Levine-Birnbaum analysis attention was focused on binary encounters. The depolarization of the incident radiation was shown to stem from the transient polarizability anisotropy of the quasimolecule. A model for the anisotropic polarizability was invoked and the dynamics was taken to be that of a free particle. They predicted that the depolarized light would be scattered into an exponential spectrum whose decay constant is related to the inverse duration of a collision. In the Thibeau-Oksengorn treatment attention was directed to the scattering of light by a single atom. A statistical analysis of the effect of perturber atoms was carried out. Thus the incident field on given atom was taken to be the sum of the externally applied wave and a fluctuating environmental field. The two theories bear a relationship to each other reminiscent of that between dynamical and statistical theories of line broadening.

Experimental studies of the spectrum by McTague and Birnbaum[3,4] have verified many of the theoretical predictions. Recent experiments by Slusher, Surko, and Strautins,[5] however, have revealed a somewhat puzzling character to the spectrum of depolarized scattered light. The wings of the spectrum do not seem able to be fitted by a single exponential curve. Rather, if plotted semilogarithmically versus frequency, there is a gradually curving slope—steep at low frequencies and less steep at higher frequencies. The data of McTague and Birnbaum also display a nonexponential character, although it is not clear from their work what significance is to be attached to it. The object of the present paper will be to try to understand, in a quantitative manner, the meaning of this curious feature.

Experiment[5] indicates that the curving-slope feature is not density dependent at low densities. This would tend to rule out dimers as a possible candidate for the effect. If rotational or vibrational transitions in the dimer are involved, the linewidths would depend on the lifetime of the dimer—a pressure-dependent quantity. Similarly, the intercollisional (constructive) interference effect proposed by Lewis and Van Kranendonk[6] has a bandwidth related to the inverse time between collisions and is thus density dependent.

A clue to the origin of the effect could be had if one considers hard-sphere collision trajectories instead of straight-line paths. For those encounters in which the spheres do not collide we have exactly the situation envisaged by Levine and Birnbaum.[1] For direct collisions, however, the radial coordinate experiences a discontinuity in slope as a function of time at the moment of impact. Since the anisotropic part of the polarizability, β, depends on r, it also exhibits this behavior. The intensity of the scattered radiation is proportional to the square of the Fourier transform of β [viz., Eq. (2)]. If we integrate by parts twice, we can express the

intensity as the inverse fourth power of the frequency shift multiplied by the Fourier transform of the second derivative of β. This second derivative contains a δ function in time, so the Fourier transform will have a part which is constant. Thus in the far spectral wings the line shape will fall off as a power and not exponentially. For a sharp repulsive potential which is analytic we no longer expect a power law but we do expect the wings to be more extended than for the case with no potential at all. Thus we see the main progenitor of the varying slope appearing, namely, the scattering process. We shall see later that the short-range part of β can also influence the slope of the spectrum.

The need for including collisional effects was originally recognized in the Thibeau-Oksengorn theory.[2] The emphasis of their paper was placed mainly on low frequencies—as is evidenced by their choice of a hard-sphere potential. As we shall see, the slope of the high-frequency spectrum is rather sensitive to the details of the potential. The present work may thus be regarded as a generalization of their work to a realistic potential.

While it is quite possible that quantum effects might lead to some oscillatory structure in the spectrum, these effects would probably be small and will be neglected in this paper. Thus classical trajectories will be employed. This would have the effect of averaging out any quantum structure.

We will proceed in a stepwise manner, investigating the effects of various complications one at a time. Thus we start with a simple form for β and a purely repulsive potential. Afterwards an attractive potential is added and its effects discussed. Finally the model for β is refined. A comparison with existing experiments will not be made in this paper. We shall assume throughout that the pressure of the gas is low enough so that only binary encounters need be considered.

THEORY

Lacking detailed molecular calculations describing the nature of the polarizability tensor, we are somewhat in the dark as to where to start. We shall begin with a very simple model, extract its consequences, and then refine it. At large interatomic separations the pair of atoms can be shown to give rise to an anisotropy[7]

$$\beta = 6\alpha^2/r^3 \ . \tag{1}$$

Since for the rare gases chemical effects are unimportant, one does not expect a major redistribution of charge in the interacting atoms and so the polarizability should not differ very much from the above expression. This model differs from that employed by Levine and Birnbaum,[1] who chose a Gaussian-like form.

Using elementary relations, the rate of collision-induced light scattering due to binary encounters can be written as

$$\frac{dI}{d\Omega} = \frac{\omega^4 I_0}{\pi c^4}\frac{n^2 v}{2}\int d\sigma \left| \int_{-\infty}^{\infty} e^{i(\omega-\omega_0)t}\alpha_{zx}(t)\,dt \right|^2 \ . \tag{2}$$

We have taken the incident beam of intensity I_0 and frequency ω_0 to propagate along the x axis with polarization directed along the z axis. The scattered radiation is observed along the z axis without regard for polarization. The frequency of the scattered light has been denoted by ω. The density of atoms in n and the relative velocity is v. After a suitable average over all orientations of the collision plane has been made this reduces to

$$\frac{dI}{d\Omega} = \frac{2I_0}{75}\left(\frac{\omega}{c}\right)^4 n^2 v \sum_{\lambda} |Y_{2\lambda}(\pi/2, 0)|^2 \times \int d\sigma \left| \int_{-\infty}^{\infty} e^{i(\omega-\omega_0)t}\,\beta(r)\,e^{i\lambda\Phi}\,dt \right|^2 \ . \tag{2'}$$

The collision plane has been chosen as the $\theta = 0$ plane. The trajectory is then described by the radial coordinate r and the azimuthal coordinate ϕ.

The key to the problem is to evaluate the scattering integral

$$I_\lambda = \int_{-\infty}^{\infty} \beta(r) e^{i(\Delta t + \lambda\phi)}\,dt \ , \tag{3}$$

where $\Delta = \omega - \omega_0$ is the frequency shift from line center. We are particularly interested in the far wings of the line, where Δ is large. Thus we shall make an asymptotic expansion of I_λ in powers of $1/\Delta$. Before this can be accomplished, however, the dynamics of the problem must be introduced. While, in principle, we could integrate Newton's equations of motion to obtain the trajectory, we shall adopt a simpler approach. The high-frequency wings of I_λ will be sensitive to the sharpest features in the scattering process. These occur near the turning point of the trajectory. Not only is the trajectory varying most rapidly there, but the function β is peaking most rapidly also. Thus all we really need to know is the behavior of the trajectory near the turning point.

The turning point is the positive root r_0 of the equation

$$\tfrac{1}{2}mv^2(1 - b^2/r_0^2) - V(r_0) = 0 \ , \tag{4}$$

where b is the impact parameter, $V(r)$ is the potential, and $\frac{1}{2}mv^2$ is the reduced kinetic energy. We have in mind, for the present, a repulsive potential, so that Eq. (4) has only one positive root. The trajectory is now expanded in the neighborhood of the turning point. From the symmetry of an orbit in a central field it follows that r and ϕ are

even and odd series, respectively. Thus

$$r = r_0 + \ddot{r}_0 \tfrac{1}{2} t^2 + \cdots = r_0 + F_0 t^2/2m + \cdots , \quad (5a)$$

$$\phi = \dot{\phi}_0 t + \cdots = vbt/r_0^2 + \cdots , \quad (5b)$$

where

$$F_0 = -\frac{\partial}{\partial r}\left(V + \frac{mv^2b^2}{2r^2}\right)\Big|_{r_0} . \quad (6)$$

F_0 is the sum of the interatomic and centrifugal forces acting at the turning point. Equation (5b) follows directly from angular momentum conservation.

Equations (5a) and (5b) are not appropriate for our use as they stand. To cast them into a more useful form one must consider the analytic behavior of r and ϕ. For each trajectory there exist two possible directions to traverse it: the forward way and the time-reversed way. This implies that r and ϕ should be double-branched functions in time. We would like to rewrite Eqs. (5a) and (5b) in a manner which would reflect this property. To order t^2 we have the equations

$$r = r_0[1 + (F_0/mr_0)t^2]^{1/2} \equiv (r_0/\xi_0)(t^2 + \xi_0^2)^{1/2} \quad (7a)$$

and

$$\sin\phi = bvt/r_0 r , \quad (7b)$$

where $\xi_0 = (mr_0/F_0)^{1/2}$. The quantity ξ_0 is a measure of the duration of a collision. In the free-particle limit the turning radius becomes the impact parameter, i.e., $r_0 \to b$. Thus $\xi_0 \to b/v$, $r \to (b^2 + v^2t^2)^{1/2}$, and $\sin\phi \to vt/r$. These are just what one would get for a straight-line trajectory. Equations (7a) and (7b) form a "pseudodynamics" which should be useful in a broad class of problems.

In the complex t plane, r has branch points at $t = \pm i\xi_0$. For a strongly repulsive potential ξ_0 can be quite different from b/v but plays an analogous role to it in determining the bandwidth of the scattered radiation, as we shall see. The following formulas (valid to the same degree of approximation) will be useful:

$$\sin^2\phi = b^2v^2t^2/r_0^2r^2 , \quad (8a)$$

$$\cos^2\phi = bvt/r^2 , \quad (8b)$$

$$\sin\phi\cos\phi = (r_0^2/r^2)[1 + t^2(1/\xi_0^2 - b^2v^2/r_0^4)] . \quad (8c)$$

These expressions also obey the above-cited correspondence principle when $V \to 0$.

The particular models that we will be looking at have $\beta(r)$ an analytic function of r everywhere except at $r = 0$.[8] Then β will be an analytic function of t except on the cuts, which will be taken to run from $i\xi_0$ to $i\infty$ and from $-i\xi_0$ to $-i\infty$. As $|t| \to \infty$ in the upper half-plane, $e^{i\Delta t}$ vanishes exponentially, $\beta \to 0$, and $\phi \to$ const. Thus an infinite semicircle in the upper half-plane, taken as a contour, would give no contribution. Consequently the trajectory may be distorted to wrap around the upper cut—going from $+i\infty - \epsilon$ to $+i\infty + \epsilon$ swinging beneath $i\xi_0$. Equation (3) becomes

$$I_\lambda = \int_c \beta(r)\, e^{i(\Delta t + \lambda\phi)}\, dt . \quad (9)$$

We can already see the origin of the "exponential" line shape in Eq. (9). Since the contour starts at $t = i\xi_0$ and extends upwards, an over-all factor $e^{-\Delta\xi_0}$ may be extracted. The remaining integral will be a much smoother function of Δ. For this reason we see that the "exponential" shape is really quite model independent.

To proceed further we introduce the specific form for $\beta(r)$ of Eq. (1). With an eye towards generalization let us write[9]

$$\beta(r) = \sum_n \beta_n (1/r^{2n+1}) , \quad (10a)$$

with

$$\beta_1 = 6\alpha^2 . \quad (10b)$$

Equation (9) can then be written as

$$I_\lambda = \sum_n \beta_n I_\lambda^{(n)} , \quad (11)$$

with

$$I_\lambda^{(n)} = \int_c \frac{e^{i(\Delta t + \lambda\phi)}}{r^{2n+1}}\, dt . \quad (12)$$

Employing Eq. (8), this becomes

$$I_0^{(n)} = \int_c \frac{e^{i\Delta t}}{r^{2n+1}}\, dt , \quad (13a)$$

$$I_{\pm 2}^{(n)} = \int \frac{e^{i\Delta t}}{r^{2n+1}} \left\{ \left(\frac{r_0}{r}\right)^2 + \left(\frac{t}{r}\right)^2 \times \left[\left(\frac{r_0}{\xi_0}\right)^2 - 2\left(\frac{bv}{r_0}\right)^2\right] \pm \frac{2ibvt}{r^2} \right\} dt . \quad (13b)$$

Equation (13b) can be rewritten as

$$I_{\pm 2}^{(n)} = \left[1 - 2\left(\frac{bv\xi_0}{r_0^2}\right)^2 \mp \frac{bv\Delta}{n + \frac{1}{2}}\left(\frac{\xi_0}{r_0}\right)^2\right] I_0^{(n)} + 2\left(\frac{bv\xi_0}{r_0}\right)^2 I_0^{(n+1)} . \quad (13b')$$

The $I_0^{(n)}$ are expressible as modified Bessel functions[10]:

$$I_0^{(n)} = \frac{2(\sqrt{\pi})\xi_0}{\Gamma(n + \frac{1}{2})}\left(\frac{1}{2}\right)^n \left(\frac{1}{r_0}\right)^{2n+1} (\xi_0\Delta)^n K_n(\xi_0\Delta) . \quad (14)$$

For high frequencies this can be expressed as

$$I_0^{(n)} = \frac{2\pi\Delta^{n-1/2}}{\Gamma(n + \frac{1}{2})}\left(\frac{1}{2\xi_0}\right)^{n+1/2} \left(\frac{\xi_0}{r_0}\right)^{2n+1} e^{-\Delta\xi_0}(1 + \cdots) \quad (\text{for } \Delta\xi_0 \gg 1) . \quad (14')$$

Having evaluated the scattering integral, we are

still faced with the integration over all impact parameters. It is convenient to transform the integration so it corresponds to an integration over distances of closest approach. From Eqs. (4) and (6) it follows that

$$d\sigma = 2\pi b db = (2\pi r_0^2 F_0/mv^2)\, dr_0 \ . \tag{15}$$

The range of integration extends from $r_0 = a$ to $r_0 = \infty$, where a is the root of

$$0 = 1 - (2/mv^2) V_0(a) \ . \tag{16}$$

Physically a corresponds to the distance of closest approach for a head-on collision.

For the repulsive potential the truncated Lennard-Jones form was adopted:

$$V(r) = 4\epsilon(\sigma/r)^{12} \ . \tag{17}$$

Then from Eqs. (4), (6), and (16) we obtain

$$F_0 = (40\epsilon/\sigma)(\sigma/r_0)^{13} + mv^2/r_0 \ , \tag{18a}$$

$$a = (8\epsilon/mv^2)^{1/12}\sigma \ , \tag{18b}$$

$$b = r_0[1 - (8\epsilon/mv^2)(\sigma/r_0)^{12}]^{1/2} \ . \tag{18c}$$

The scattered intensity may be written as

$$\frac{dI}{d\Omega} = \frac{3I_0}{5}\left(\frac{\omega\alpha}{c}\right)^4 \frac{n^2 J}{m} \ , \tag{19a}$$

where J is defined by

$$J = \frac{1}{v}\int_a^\infty dr_0 r_0^2 F_0[(I_0^{(1)})^2 + \tfrac{3}{2}(I_2^{(1)})^2 + \tfrac{3}{2}(I_{-2}^{(1)})^2] \ . \tag{19b}$$

If we work in units such that $\epsilon = \sigma = m = 1$, then J will be a universal function valid for all gases.[11]

The extension to the case where an attractive potential is included can be carried out straightforwardly. We have now in place of Eq. (17) the potential

$$V(r) = 4\epsilon[(\sigma/r)^{12} - (\sigma/r)^6] \ . \tag{20}$$

Instead of Eq. (18a) we obtain

$$F_0 = \frac{40\epsilon}{\sigma}\left(\frac{\sigma}{r_0}\right)^{13} - \frac{16\epsilon}{\sigma}\left(\frac{\sigma}{r_0}\right)^7 + \frac{mv^2}{r_0} \ , \tag{21a}$$

while Eq. (18b) becomes

$$a = \sigma\{\tfrac{1}{2}[1 + (1 + mv^2/2\epsilon)^{1/2}]\}^{-1/6} \ . \tag{21b}$$

Finally, Eq. (18c) becomes

$$b = r_0\left\{1 - \frac{8\epsilon}{mv^2}\left[\left(\frac{\sigma}{r_0}\right)^{12} - \left(\frac{\sigma}{r_0}\right)^6\right]\right\}^{1/2} \ . \tag{21c}$$

An additional feature appears in the range of integration, however. This is due to the fact that for fixed b, r_0 may undergo a discontinuity as v is raised above a certain critical value. This is because the repulsion mechanism is suddenly switched from being the centrifugal force to the repulsive force. Thus the range of integration on r_0 may split up into two disjoint segments. This is discussed further in Appendix A.

We now try to refine our model for β somewhat beyond the asymptotic expression of Eq. (1). The next term in the asymptotic series will be included and the series will be truncated here.[9] Thus we take

$$\beta = 6\alpha^2(1/r^3 + \rho/r^6) \ , \tag{22}$$

where ρ is a number to be evaluated. We shall compute the Kerr constant corresponding to Eq. (22) and compare it with the experimental values of Buckingham and Dunmur.[12] They have evaluated theoretical Kerr constants for the model of Eq. (1) and found considerable disagreement between theory and experiment. It is apparent that higher-order terms, such as that included in Eq. (22), could reduce the discrepancy. By truncating the series we are assuming that most of the deviation lies in the second term.

The Kerr constant is given by

$$B_K = \frac{8\pi^2 N^2}{405kT}\int_0^\infty \beta^2 r^2 e^{-V/kT}\, dr$$

$$= \sum_{mn} \beta_n \beta_m I_{mn} \ , \tag{23}$$

where

$$I_{mn} = \int r^{-2n-2m} e^{-V/kT}\, dr \ . \tag{24}$$

We are temporarily employing the notation of Eq. (10a) for convenience. Here N is Avogadro's number. By letting $u = (\sigma/r)^6$ and $\nu = \frac{1}{3}(n + m - \frac{1}{2})$

$$I_{mn} = \tfrac{1}{6}\sigma^{1-2n-2m}\int_0^\infty du\, u^{\nu-1} e^{-\gamma(u^2-u)} \ , \tag{25}$$

where $\gamma = 4\epsilon/kT$. This, in turn, can be expressed in terms of parabolic cylinder functions.[13] Thus

$$I_{mn} = \tfrac{1}{6}\sigma^{1-2n-2m}(2\gamma)^{-\nu/2}\Gamma(\nu)\, e^{\gamma/8} D_{-\nu}((\tfrac{1}{2}\gamma)^{1/2}) \tag{26}$$

(Buckingham and Dunmur express I_{11} in terms of the H_6 function, which, as we see, is proportional to the parabolic cylinder function.) Thus, letting $g = (\frac{1}{2}\gamma)^{1/2}$, we have

$$B_K = B_K^0\left(\frac{(2x/\pi)(2\gamma)^{-1/4}[V(\frac{1}{2},g)\pi - U(\frac{1}{2},g)]}{V(0,g)} + \frac{x^2(2\gamma)^{-1/2}V(1,g)}{V(0,g)}\right) \ . \tag{27}$$

The U and V functions are tabulated by Abramowitz and Stegun.[14] B_K^0 is the Kerr constant for the model of Eq. (1) and is given by

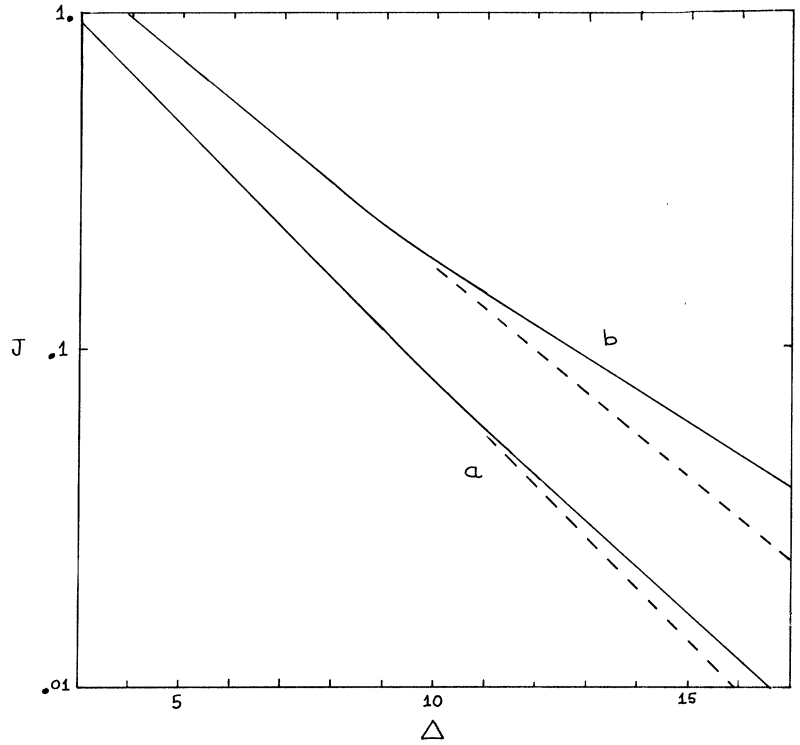

FIG. 1. J vs Δ for two cases ($v = 2.74$). In curve a, a truncated repulsive Lennard-Jones potential was employed, while in curve b the regular Lennard-Jones potential was used. The dashed lines represent asymptotes to the low-frequency slopes.

$$B_K^0 = (4\pi^3 N^2/1215kT\sigma^3)(6\alpha^2)^2(2\gamma)^{-1/4} e^{\gamma/8} V(0,g) \ . \tag{28}$$

By comparing Eq. (27) to experiment we are able to extract a value for σ. We can then use Eq. (11) to obtain a refined scattering integral. The remainder of the analysis proceeds exactly as before.

RESULTS AND DISCUSSION

In the previous sections a theory for the asymptotic line shape of collision-induced light scattering has been presented. This theory is relevant only to the non-near wings of the scattered spectrum and is probably unreliable for $\Delta \lesssim 3$. [To express Δ in cm^{-1} we multiply by $(\epsilon/m)^{1/2}/2\pi c\sigma$.] In order to obtain a theory valid near the line center one would undoubtedly need to include the dynamics in a more sophisticated manner. Thus one would have to determine the role played by dimers,[15] evaluate the effect of the intercollisional interference,[6] and include the dynamics of two-body collisions in more detail. For the asymptotic line shape, however, we were able to simplify the description considerably. The key to this simplification lies in the introduction of a pseudodynamics which respects the analytic behavior of the trajectory in the complex time plane.

The present theory applies directly to the Stokes side of the spectrum. To obtain the appropriate line shape for the anti-Stokes side one must include the additional Boltzmann factor $e^{-\hbar\Delta/kT}$.

In order to compare the theory with experiment it is still necessary to perform an average over the thermal distribution of velocities. To this end the distribution function

$$f(v) = (2\pi)^{1/2}\tau^{-3/2} v^2 e^{-v^2/2\tau} \tag{29}$$

is employed, where $\tau = kT/\epsilon$. The effect of velocity averaging turns out not to be very significant, affecting the curvature of the logarithm of the spectrum only slightly.

We now apply the theory to some practical cases. We shall be concerned here only with the rare gases, as most of the experimental work has focused on these. The theory may readily be extended to more complicated systems.

Argon

Let us first try to determine what effect, if any, the potential form has on the line shape. We begin by considering a purely repulsive potential of the form of Eq. (17). The model for β will be taken simply as the asymptotic form given in Eq. (1). In Fig. 1, J is plotted as a function of Δ for a fixed $v = 2.74$ units. (We are neglecting thermal averaging in this computation. The speed is the mean relative speed of a colliding argon pair at $T = 300\,^\circ$K.) Note that the spectrum may be characterized quite accurately as being piecewise exponential. Only two slopes appear on a semilogarithmic

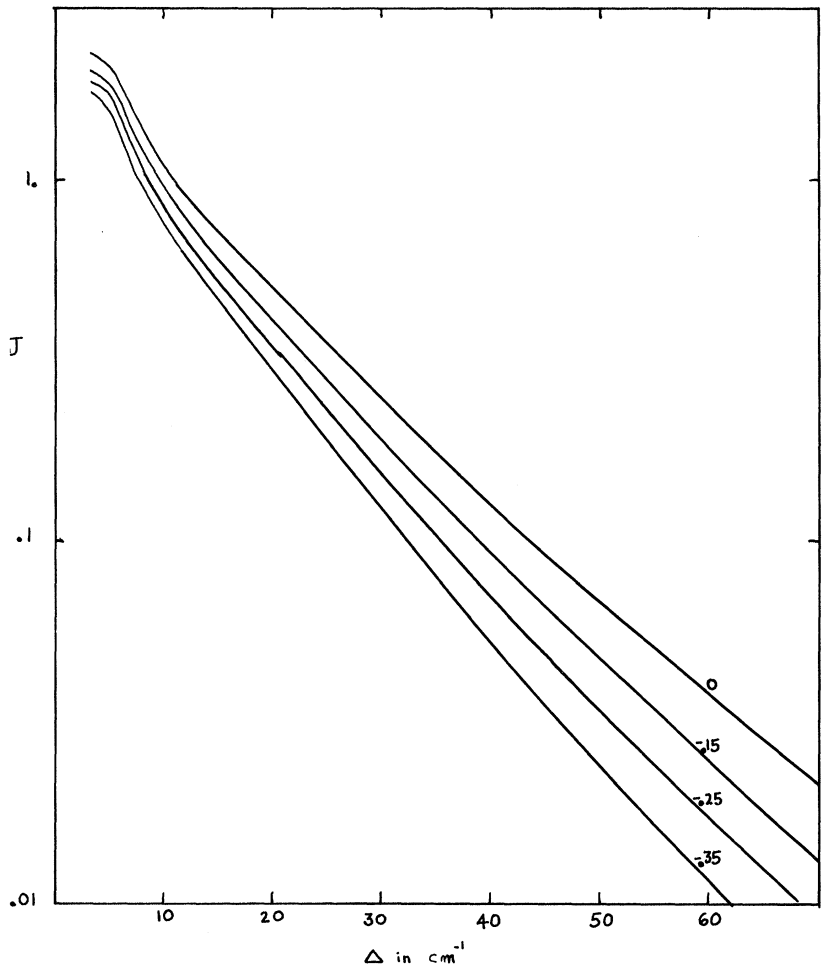

FIG. 2. J vs Δ for several different assumed Kerr constants in Ar. The curve $x=-0.25$ corresponds to the observed experimental value (thermal averaging included).

plot. If J is expressed in the form $J=Ce^{-\Delta/\delta}$, then δ represents a characteristic inverse decay length. The low-frequency region has $\delta=9.8$ cm^{-1}, while the high-frequency region has $\delta=11$ cm^{-1}. The break occurs at roughly 28 cm^{-1}. In this analysis for argon we have taken[16] $\epsilon/k=119.8$ °K and $\sigma=3.405$ Å.

The existence of two distinct spectral regions can be understood by noting that there exist two different types of collisions. Those collisions with the repulsive core, being quite sharp, generate high-frequency Fourier components, thereby influencing the outer wings of the spectrum. On the other hand, as one goes to smaller frequencies the effect of soft distant collisions becomes more manifest.

We next retain the model employed for β and use a potential of the form of Eq. (20). Although we have included an attractive potential, it has the effect of altering the repulsive force also, as it lowers the distance of closest approach. In addition, it increases the velocity of the particles prior to the moment of impact due to the acceleration of the attractive force. Consequently the duration of a collision ξ_0 will be decreased. Thus a large bandwidth, measured by δ at high frequencies, is to be expected. Furthermore, one expects the attractive force to cause more collisions with the repulsive core than before. This will tend to increase the relative importance of core collisions to distant collisions. In Fig. 1 we present the J-vs-Δ curve for the same physical parameters as in the previous case. The low-frequency δ is 15.5 cm^{-1}. Instead of having two slopes it now seems possible to characterize the spectrum by three slopes—the intermediate δ being 13.0 cm^{-1}. The effect of the potential is thus rather important. The inclusion of the attractive potential has introduced a new bend in the spectrum and the high-frequency slope has been changed considerably. By including a negative (attractive) term in the potential the total potential curve is altered in both the attractive and repulsive regions. It is the alteration in the repulsive region which primarily influences the high-frequency slope. The low-frequency slope, on the other hand, has not been radically altered, indicating that it is associated with the distant collisions. We shall see

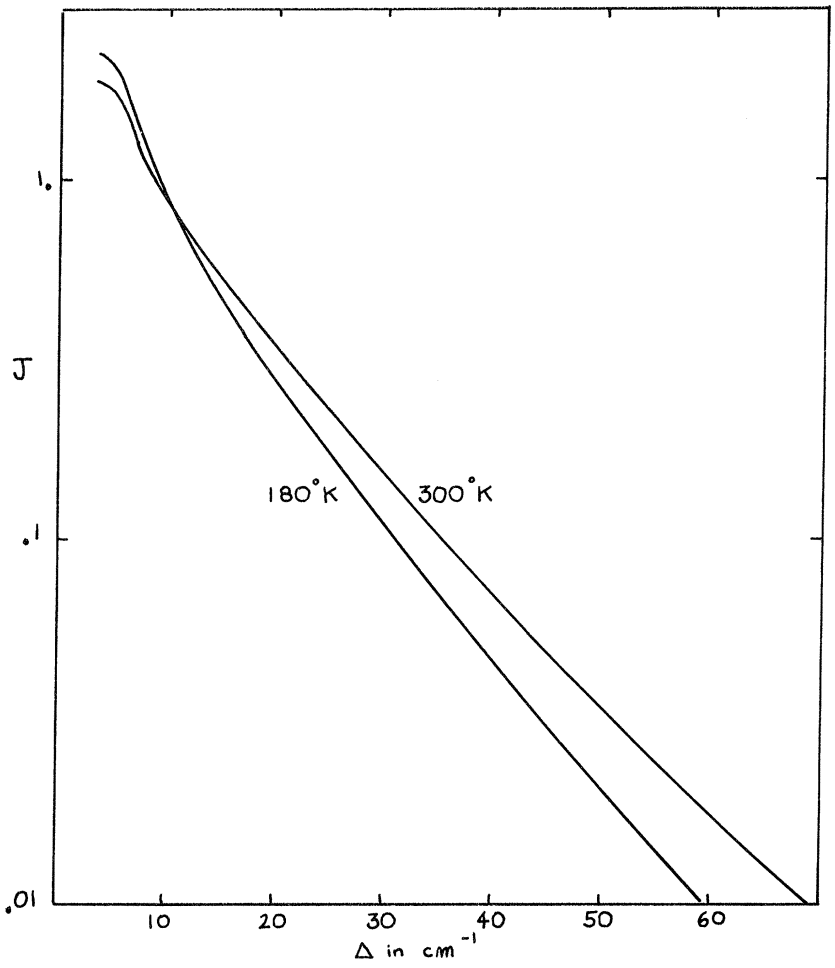

FIG. 3. J vs Δ for argon at two temperatures (thermal averaging included).

shortly that the high-frequency slope can be obtained directly by just considering close collisions.

In order to obtain a rough idea of just how sensitive the high-frequency slope is the potential form, consider the following. Let us typify a close collision by a head-on encounter. For r_0 we simply take a. As noted earlier, the asymptotic character of the line shape is determined mainly by the location of the branch point in the upper half-plane. From Eqs. (14′) and (2′) it follows that

$$\delta \sim 1/2\xi_0(a) . \tag{30}$$

For the sake of definiteness, again, we consider argon at room temperature and neglect thermal averaging. We obtain $\delta = 16.2\ \mathrm{cm}^{-1}$ for the Lennard-Jones potential, which compares rather favorably with the numerical result of $15.5\ \mathrm{cm}^{-1}$ found earlier. If we try other "realistic" potential forms, we find $\delta = 17.5$ for a Saxena modified Buckingham (exponential-6) potential[16] and $\delta = 15.7$ for a Buckingham corner potential[16] (with their β parameter = 0.2). Thus one could realistically expect a variation in the slope of as much as ± 1 cm as one potential form is substituted for another. This variation reflects primarily the behavior near the turning point.

It should perhaps be emphasized that the asymptotic slope, as given in Eq. (30), is valid at asymptotically high-frequency shifts. Since we only calculate the spectrum up to some finite, but high frequency, we ought to expect residual sensitivity to those aspects of the problem other than the repulsive part of the potential. In fact, our calculations show a slight sensitivity of the spectra to the ρ parameter. This could be thought of as stemming from the Fourier components generated by the radial variation of $\beta(R)$. Since this variation is not as dramatic as that of the potential, we should expect this residual sensitivity to diminish as we probe higher-frequency shifts.

Our final task is to study the influence of the short-range part of β on the spectral shape. To this end we employ the truncated asymptotic form described in Eq. (22). The parameter ρ can then be varied. There exists a particular ρ which reproduces the experimental Kerr constant, viz.,

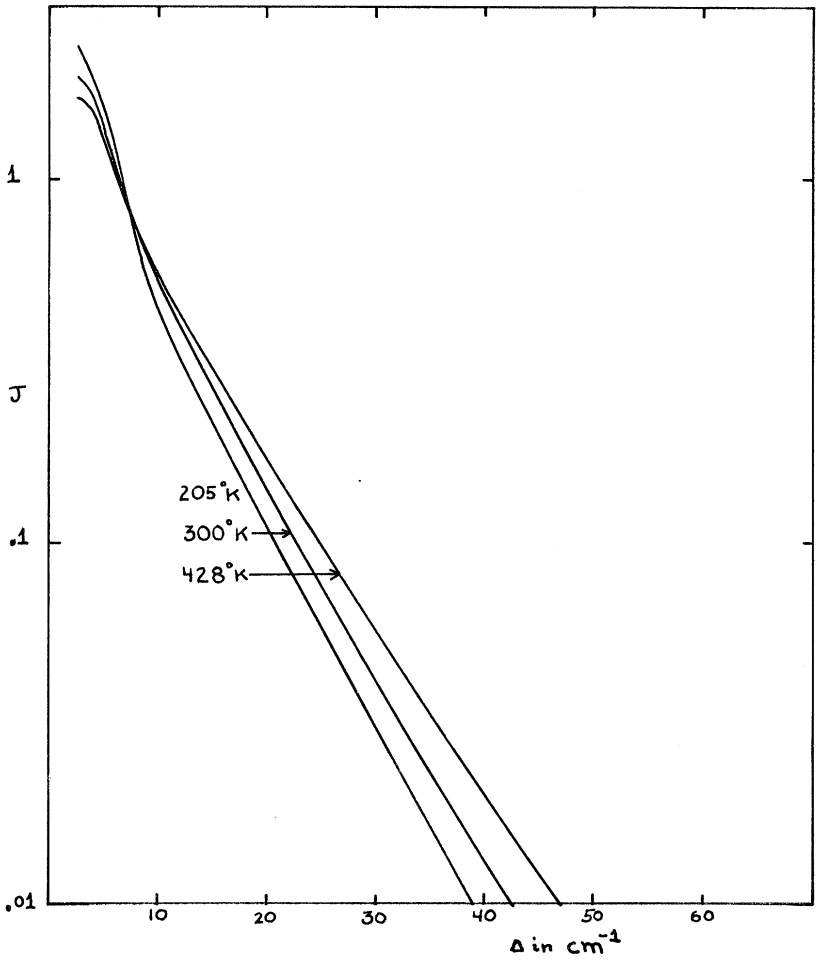

FIG. 4. J vs Δ for krypton at three temperatures (thermal averaging included).

Eqs. (27) and (28). This gives[17] $\rho = -0.25\sigma^3$. The experimental error limits on the Kerr constant[12] allow us to define a range for the parameter ρ which is physically acceptable. This range is bounded by roughly $-0.15\sigma^3 > \rho > -0.35\sigma^3$. In Fig. 2 we have plotted the spectral integral J as a function of Δ for these values of ρ. In this figure thermal averaging has been included. The value of $\rho = 0$, corresponding to the model of Eq. (1), is also included for the sake of comparison. We note that as $|\rho|$ is increased, the spectral integral J becomes smaller. This is to be expected since the β function becomes smaller near the turning point. The low-frequency slope is virtually unaffected—again supporting our conclusion that it is due to the soft distant collisions. The slopes at intermediate and high frequencies are influenced, however.

We note that the actual spectral shape is rather sensitive to the value of the Kerr constant, particularly at high frequencies. This could potentially provide us with a means to obtain this quantity by making an optimal fit to the experimental data. For argon it turns out[5] that experiment and theory agree rather well with the experimental value quoted by Buckingham and Dunmur.[12]

In Fig. 3 we have drawn the spectral integral for two values of the temperature. We note that at high frequencies the high-temperature spectrum lies above the low-temperature spectrum. This again can be understood as a consequence of having more rapid collisions at the elevated temperature, thereby producing more of a contribution to the far spectral wings.

Krypton

The analysis for krypton proceeds in much the same way as for argon. The Lennard-Jones parameters were taken to be[16] $\epsilon/k = 171\ ^\circ\mathrm{K}$ and $\sigma = 3.6$ Å and the Kerr constant was taken to be that measured by Buckingham and Dunmur,[12] despite the large experimental uncertainty. Theoretical line shapes are presented in Fig. 4 for a few values of temperature. The value of ρ turned out to be $-0.38\sigma^3$.

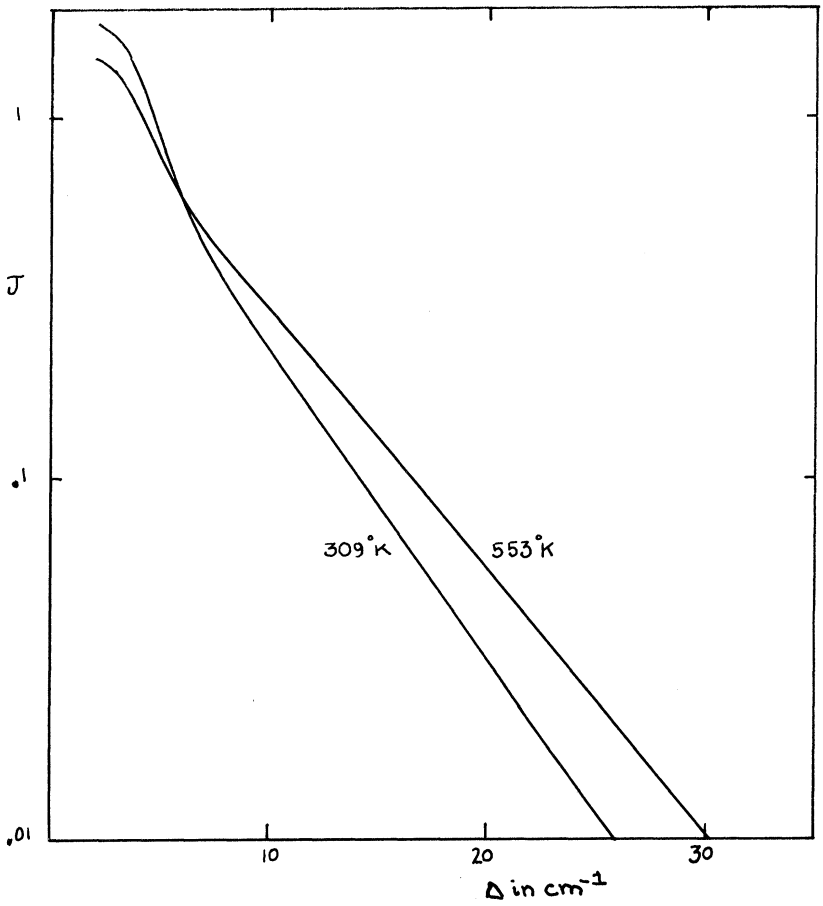

FIG. 5. J vs Δ for xenon at two temperatures (thermal averaging included).

Xenon

For xenon the Lennard-Jones parameters $\epsilon/k = 221\ ^\circ\mathrm{K}$ and $\sigma = 4.1$ Å were employed,[16] and the experimental Kerr constant[12] was accepted. The results are presented in Fig. 5. Here $\rho = -0.57\sigma^3$.

CONCLUSION

In conclusion, we have developed in this article a classical theory for the line shape of collision-induced scattered light, quantum effects being deferred for discussion in another article. We found the line shape to be governed by several different atomic collision parameters, such as the interatomic potential parameters and the parameters determining the form of $\beta(r)$. The latter quantities could be related to the static Kerr constant. Considering the crude models adopted for β and V, we really should not expect perfect agreement between theory and experiment. Thus one might expect some degree of sensitivity to the form of the potential curve near the turning point [which is really only guessed at in the Lennard-Jones form, Eq. (20)]. Viewed from a different aspect, CIS could potentially provide one with a method for studying the detailed aspects of the potential in this region. This would provide complementary information to that obtained from viscosity data. These data usually are sensitive to a combination of the repulsive and long-range attractive parts of the potential. Parts of CIS, however, are sensitive mainly

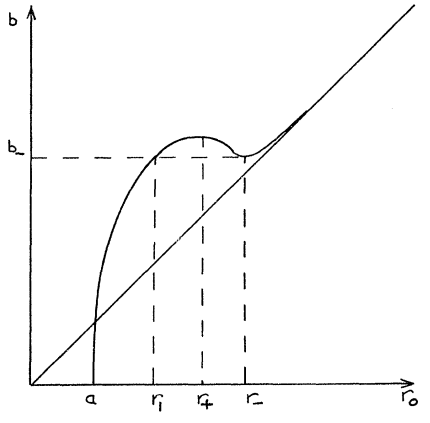

FIG. 6. Impact parameter versus distance of closest approach for an attractive potential for case $mv^2 < 1.6\epsilon$.

to the repulsive region. Before this can be implemented, however, we must obtain better knowledge of the β function. Thus *ab initio* calculations of β would be very helpful—even if only the ρ coefficients were computed.

ACKNOWLEDGMENTS

We would like to thank Dr. R. E. Slusher and Dr. C. M. Surko for making available to us their experimental results prior to publication and for many interesting discussions. We also would like to thank Dr. A. A. Abrahamson for an informative discussion concerning interatomic potentials.

APPENDIX A

In this appendix we describe how the range of integration over dr_0 breaks up into two segments when an attractive force is present. From Eq. (15) we have

$$\frac{db}{dr_0} = \frac{r_0^2}{b}\frac{F_0}{mv^2} \quad , \tag{15'}$$

which tells us that the extrema of $b(r_0)$ occur when F_0 vanishes. For the potential of Eq. (20) the roots to $F_0 = 0$ are at

$$r_0 = \sigma\left[\tfrac{1}{5} \pm \left(\tfrac{1}{25} - mv^2/40\epsilon\right)^{1/2}\right]^{-1/6} \equiv r_\pm \ . \tag{A1}$$

For $mv^2 > 40\epsilon/25$ there are no real roots to this equation. Then b is a monotonic function of r_0 and no breakup of the region occurs. r_0 simply varies from a to ∞.

For $mv^2 < 40\epsilon/25$, however, two real roots exist, which will be denoted by $r_\pm$. r_+ corresponds to a relative maximum in the $b(r_0)$ curve, while r_- is a relative minimum. Let V_- be defined by

$$V_- = V(r_-) = 4\epsilon\left[(\sigma/r_-)^{12} - (\sigma/r_-)^6\right] \ . \tag{A2}$$

The impact parameter corresponding to r_- is b_-, where

$$b_- = r_-\left[1 - (2/mv^2)V_-\right]^{1/2} \ . \tag{A3}$$

Finally, we define r_1 as the other root to the equation

$$b_-^2 = r_1^2 - (2/mv^2)V(r_1) \ . \tag{A4}$$

The region of integration breaks up into (a, r_1) and (r_-, ∞). These results are summarized in Fig. 6.

As a first approximation we can take $r_1 = a$. When inserted in Eq. (A4), we obtain a refined guess,

$$r_1 = \sigma\left\{\tfrac{1}{2} + \left[1 - (mv^2/2\epsilon)(b_-^2/a^2 - 1)\right]^{1/2}\right\}^{-1/6} \ . \tag{A5}$$

The breakup occurs because that part of the repulsive potential below the centrifugal hump in the effective potential is classically inaccessible.

APPENDIX B

The intensity distribution in frequency and angle of the energy radiated by an accelerating charge distribution is given by the formula[18]

$$\frac{dI_\epsilon}{d\Omega} = \frac{\omega^2}{4\pi^2 c^3} \times \left| \int_{-\infty}^{\infty} dt \int d\vec{x}\, \hat{\epsilon}\cdot\hat{n}\times(\hat{n}\times\vec{J}) e^{i\omega(t - \vec{n}\cdot\vec{x}/c)} \right|^2 \ , \tag{B1}$$

where $\hat{n}$ is a unit vector from a source point to the field point, $\vec{J}$ is the current density, and $\hat{\epsilon}$ is a polarization vector. Since the interaction region is small compared to an optical wavelength, we shall make the dipole approximation. The integrated current density may be related to the time rate of change of the dipole moment, which in turn may be related to the electric field. Thus

$$\frac{dI_\epsilon}{d\Omega} = \frac{\omega^4}{4\pi^2 c^3}\left| \int_{-\infty}^{\infty} dt\, \hat{\epsilon}\cdot\hat{n}\times(\hat{n}\times\overleftrightarrow{\alpha}\cdot\vec{E}) e^{i\omega t} \right|^2 \ , \tag{B2}$$

where $\overleftrightarrow{\alpha}$ is the polarizability tensor. Upon multiplying this by the collision rate/volume for collision with impact-parameter area $d\sigma$, $\frac{1}{2}n^2 v\, d\sigma$, we obtain Eq. (2).

---

[1] H. B. Levine and G. Birnbaum, Phys. Rev. Letters 20, 439 (1968).

[2] M. Thibeau and B. Oksengorn, Mol. Phys. 15, 579 (1968).

[3] J. McTague and G. Birnbaum, Phys. Rev. Letters 21, 661 (1968).

[4] J. P. McTague and G. Birnbaum (unpublished).

[5] R. E. Slusher, C. M. Surko, and J. Strautins (unpublished). A preliminary account of this work has already been given by J. I. Gersten, R. E. Slusher, and C. M. Surko, Phys. Rev. Letters 25, 1739 (1970).

[6] J. Courtenay Lewis and J. Van Kranendonk, Phys. Rev. Letters 24, 802 (1970).

[7] L. Silberstein, Phil. Mag. 33, 521 (1917). The effects of induced dipoles may be included to all orders and gives $\beta = (6\alpha^2/R^3)\,(1 - \alpha/R^3 - 2\alpha^2/R^6)^{-1}$. This differs from Eq. (1) by at most 4% for argon. See also A. D. Buckingham and M. J. Stephen, Trans. Faraday Soc. 53, 884 (1957).

[8] Note that this is not true, for example, for the model of Ref. 7, which has poles at points in the r plane.

[9] The polarizability tensor for the quasimolecule is the expectation value of an even-parity operator between molecular wave functions. If these wave functions are expanded in a multipole series, we have the following terms: First-order perturbation theory gives dipole-dipole (R^{-3}). All other multipole contributions vanish. Second-order perturbation theory contains second-order dipole-dipole interaction (R^{-6}), second-order dipole-quadrupole (R^{-8}), mixed dipole-dipole and quadrupole-quadrupole (R^{-8}). Thus it is clear that the index n ranges over the values 1, $2\frac{1}{2}$, $3\frac{1}{2}$, ...

[10] As in Refs. 1 and 2.

[11] This statement remains true even when the attractive part of the Lennard-Jones potential is included.

[12]A. D. Buckingham and D. A. Dunmur, Trans. Faraday Soc. 64, 1776 (1968).
[13]I. S. Gradshteyn and I. W. Rhyzhik, *Table of Integrals, Series, and Products* (Academic, N. Y., 1965), Integral 3.462.1.
[14]*Handbook of Mathematical Functions*, edited by M. Abramowitz and I. A. Stegun, Natl. Bur. Std. (U.S.) Applied Mathematics Series–55 (U.S. GPO, Washington, D. C., 1964).
[15]J. I. Gersten and H. M. Foley, J. Chem. Phys. 45, 3885 (1966); 49, 5254 (1968).
[16]J. O. Hirschfelder, C. F. Curtiss, and R. B. Bird, *Molecular Theory of Gases and Liquids* (Wiley, New York, 1954), p. 1110.
[17]This corresponds to choosing that root of Eq. (27) which perturbs Eq. (1) the least.
[18]J. D. Jackson, *Classical Electrodynamics* (Wiley, New York, 1962), Chap. 14.

PHYSICAL REVIEW A VOLUME 4, NUMBER 1 JULY 1971

s-Wave Elastic Positron-Hydrogen Scattering in the Ionization Region

Gary Doolen*
Physics Department, Texas A & M University, College Station, Texas 77843
and
Gary McCartor†
Manned Spacecraft Center, Houston, Texas 77058
and
F. A. McDonald
Physics Department, Southern Methodist University, Dallas, Texas 75222
and
J. Nuttall*
Physics Department, Texas A & M University, College Station, Texas 77843
(Received 1 February 1971)

The method of extrapolating the t matrix from complex energies to real energies is tested on the positron-hydrogen s-wave amplitude at 29 energies in the elastic and inelastic regions, including 10 energies in the ionization region. The error in the extrapolated t matrix is not expected to be more than 10% in the ionization region.

I. INTRODUCTION

Recently a method has been proposed for computing scattering amplitudes at energies allowing final states for three charged particles.[1] In this paper we report the results of an s-wave study of this complex-energy extrapolation method applied to positron-hydrogen scattering. This method is of interest because it is the only mathematically sound and practical procedure that has been proposed to describe the scattering of three charged particles above the ionization threshold.

The first step in this method is to calculate variationally the scattering amplitude at complex energies where the calculation is known to converge. As a variational technique, we use the inhomogeneous Rayleigh-Ritz method. The results of this paper show, as expected, that the convergence rate of the variational method increases with increasing imaginary part of energy. In the case treated here, however, it is possible, even in the ionization region, to obtain good convergence surprisingly close to the real axis in energy.

It has been determined[2] that in this case the amplitude has a singularity, as the complex momentum p approaches its real physical value k, of the form $C_0 + C_1 q + C_2 q^2 + D_3 q^3 \ln q + C_4 q^3 \cdots$, where $q = p - k$. This singularity is so weak that it appears that the extrapolation from the calculated values of the amplitude to the point $p = k$ should not be too difficult, provided we keep away from thresholds and resonances. The accuracy of the extrapolation procedure might be improved by fitting the calculated amplitude with a function containing the singularity above, but we have not attempted to do this here.

First, describing our procedure in more detail, we present numerical results in the elastic and inelastic regions.

II. PROCEDURE

We use the inhomogeneous Rayleigh-Ritz variational principle given by McDonald and Nuttall[1] as follows:

$$[T(p)] = \langle \phi | V\phi \rangle + \langle \chi_t | V\phi \rangle + \langle V\phi | \chi_t \rangle - \langle \chi_t | (E - H)\chi_t \rangle ,$$

where

$$\phi = \frac{1}{2\pi} e^{-r_1} \frac{\sin kr_2}{kr_2}$$

and $E = p^2 - 1$, $k = \mathrm{Re}p$. Here, H is the Hamiltonian and V is the potential for e^+-H elastic scattering. The trial function χ_t is taken to be a sum of the form